Adaptive polymersome and micelle morphologies in anticancer nanomedicine: from design rationale to fabrication and proof-of-concept studies

Imke A.B. Pijpers†[a], Loai K.E.A. Abdelmohsen†[a], Yifeng Xia[b], Shoupeng Cao[a], David S. Williams[c], Fenghua Meng[b *], Jan C.M. van Hest[a *] and Zhiyuan Zhong[b *]

[a]Eindhoven University of Technology, P.O. Box 513 (STO 3.31), 5600MB Eindhoven, The Netherlands

[b]Biomedical Polymers Laboratory, and Jiangsu Key Laboratory of Advanced Functional Polymer Design and Application, College of Chemistry, Chemical Engineering and Materials Science, Soochow University, Suzhou 215123, PR China

[c]Department of Chemistry, Swansea University, Swansea SA2 8PP, United Kingdom

† These authors have contributed equally

1. Introduction

Structures in biology display various morphologies. Morphological characteristics, such as size and shape, are determining factors in the function of a host of nano- and microsized biomaterials. Intrigued and inspired by the intricacy of natural architectures, researchers (from various backgrounds) seek to develop artificial counterparts in order to replicate and thereby harness their function for diverse applications, from drug delivery to electronic sensing. In particular, well-defined nanoparticles with various morphologies are a great interest for biomedical research.[1] To this end, researchers are in search of a diverse molecular toolbox from which a broad range of nanoscopic architectures can be constructed with discrete properties dictated by the physicochemical attributes of their respective building blocks. Such nanoengineering is inspired by the plethora of intermolecular driving forces associated with self-assembled biological structures, which can be harnessed by the generation of synthetic, supra-molecular architectures that possess the requisite chemical versatility to facilitate application in biomedical research. The impact of morphologically discrete nanoparticles upon the development of nanomedicine is an important topic, gaining increasing attention for its potential to provide a new avenue for the development of future therapeutic technologies. Scheme 1 provides an overview of the adaptive morphologies of nanoparticles based on block copolymers in anticancer nanomedicine.

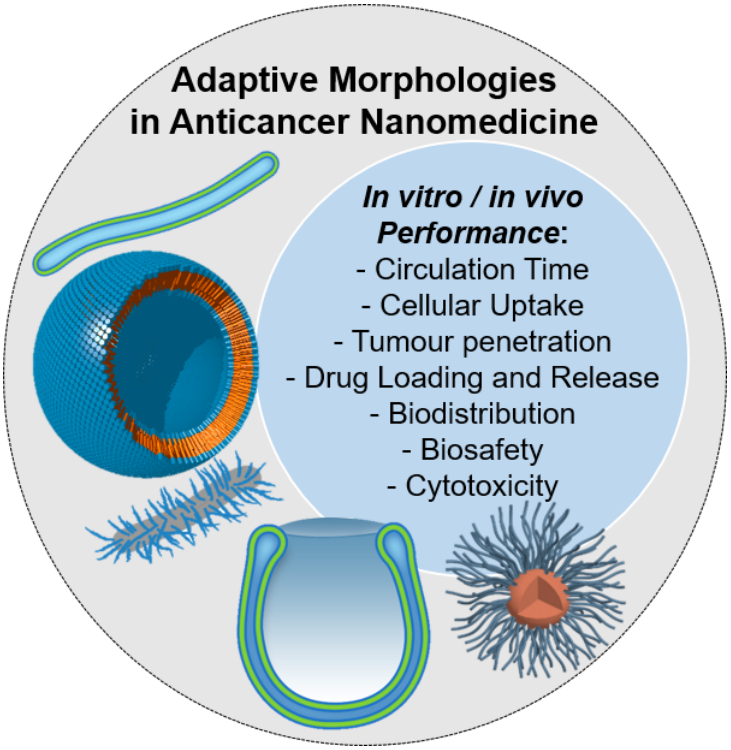

Scheme 1. Overview of adaptive morphologies in anticancer nanomedicines.

Nanomedicine focuses upon the use of nanoparticles between 1-100 nm in diameter and of broad chemical compositions to be used towards various applications in the life sciences (Figure 1). During the last decade, the field of nanomedicine has witnessed rapid growth, with promising results that indicate great potential to address challenging diseases such as cancer.

Although a large library of molecular therapeutics has been designed and deployed against cancer, due to the unsurpassable barriers of physicochemical limitations (such as low solubility and instability) or poor specificity such drugs encounter to their implementation, cancer continues to be one of the deadliest diseases affecting human health today. Conventional anticancer treatments, such as chemo- and radiotherapy, cause damage to both healthy and diseased tissue, significantly decreasing the survival rate while requiring medical reexamination. In contrast, Doxil®, a pioneering example of an effective nanomedical formulation, is a liposomal system utilizing the 'stealth' behavior of a poly(ethylene glycol)(PEG)-ylated surface along with high drug-loading capacity that was FDA-approved and brought to market in 1995.[2] More recently, Abraxane®, based on albumin-stabilized nanoparticles, has also come to market for breast cancer therapy. Although these products have spearheaded the presence of nanomedicine in the market, research continues towards the generation of functional nanotechnologies with greater efficacy *in vivo* through the optimization of morphological characteristics.

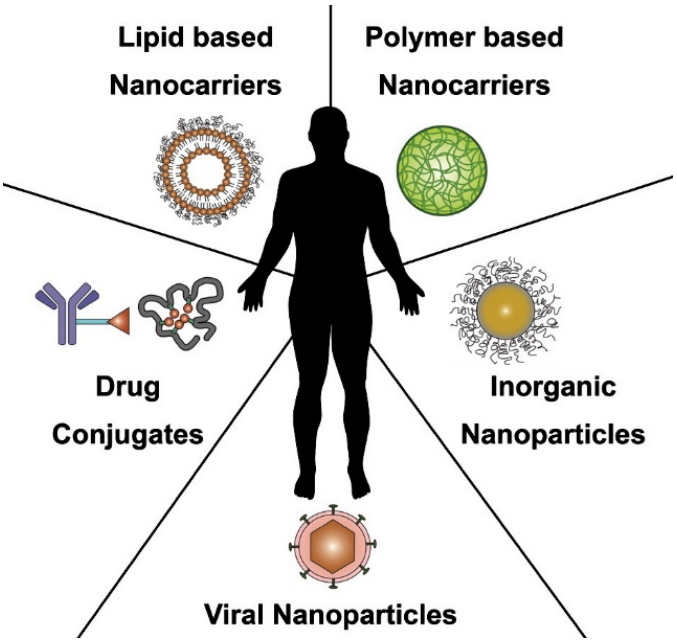

Figure 1. Schematic demonstrating the various nanoplatforms currently being studied for their therapeutic applications. Reprinted with permission from reference.[3]

One of the most well-established, beneficial properties of nanomedical formulations is their stealth-like character, which prevents clearance by renal filtration and the mononuclear phagocyte system (MPS) associated with the process of opsonization. Such processes occur shortly after nanoparticles enter the bloodstream, hindering their therapeutic efficacy and limiting their circulation time.[4] Stealth characteristics of nanoparticles can be introduced through a process called PEGylation, where poly(ethylene glycol) (PEG) is used to create a hydrophilic, low protein binding surface to reduce opsonization and thereby evade the MPS.[5] For this reason, the use of PEG as the hydrophilic block in the self-assembly of amphiphilic components is a common practice. Although the engineering of complex nanoarchitectures is not a new field, it has undergone a fundamental shift in recent years. With increasing attention being given to morphological features on the nanoscale, it is increasingly recognized that changes in the physicochemical attributes of a nanoparticle can have significant consequences for their behavior in a biological setting. In terms of particle size, relatively large nanotherapeutics are less effective at treating solid tumors due to their preferential association with peripheral cells after extravasation from adjacent blood vessels, limiting penetration and compromising efficacy.[6] Such limited tumor penetration in nanomedicine has been wildly recognized as the main hindrance in the treatment of solid tumors. Beyond the effect of particle size, which is a well-established factor, another key factor that has emerged is shape.[7] Despite their large size, red blood cells (RBCs) are able to smoothly navigate through the spleen slits because of their unique biconcave, discoidal shape and mechanical flexibility. Such a key morphological feature can be exploited in the design of nanoparticles in order to mimic the performance of RBCs, which might allow for longer distribution and decreased renal filtration.[8] Until now, there have been very few

nanoparticles with novel structures that could meet the requirements for particle size while effectively achieving both enhanced tumor accumulation/retention and deeper penetration.[6] Therefore, rationally engineering the morphological properties of nanoparticles provides a promising avenue of development to address key limitations of nanomedical technology (Figure 2).

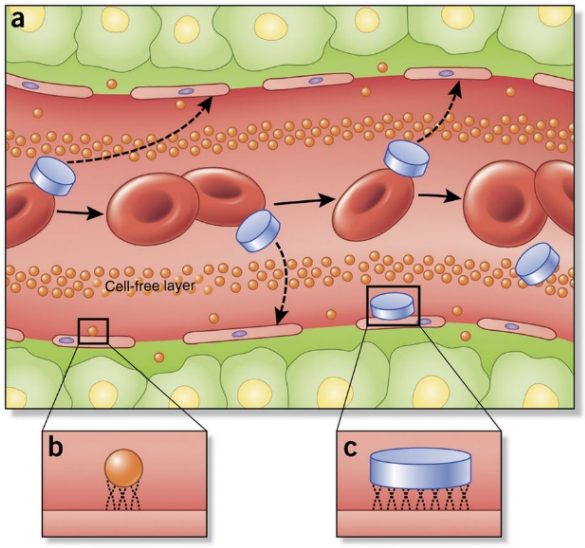

Figure 2. Intelligent particle design determines the distribution of nanoparticles in the bloodstream and their interaction with cells is tailored by their contact surface resulting from morphological features. Reprinted with permission.[7]

Successful fabrication of nanoparticles with nanomedical applications relies heavily on their ability to overcome various biological barriers. With this in mind, researchers now seek to engineer adaptive nanoparticles that are able to explore new frontiers for the development of increasingly effective nanomedical formulations. For example, the biological (immunological) response to size-controlled particles is well studied. Conventional stealth nanomedical formulations (< 400 nm) are recognized to accumulate in solid tumor regions but are poor at penetrating the dense collagen matrix, which greatly limits efficacy. Conversely, smaller nanomedicines (< 30 nm) demonstrate far more effective tumor penetration, potentially improving treatment because of a reduced diffusional hindrance. However, such particles suffer from rapid clearance by renal filtration and inferior circulation half-life time with inefficient tumor accumulation/retention because of their ability to re-enter the bloodstream.[4] Currently, research is focused on exploiting the enhanced permeation and retention (EPR) effect as a method of passively diffusing particles through the (leaky) endothelial vascular wall of tumors.[9] However, the EPR effect only occurs in fast growing tumors, severely limiting its application as a general targeting mechanism. Additionally, only a small amount of nanoparticles eventually reach the tumor tissue, fueling discussion as to whether exploitation of the EPR effect is a viable strategy for nanomedicine.[10] As opposed to passive targeting mechanisms, active targeting, using surface-bound antibodies, ligands or peptides, can be employed to selectively

direct nanoparticles towards specific tissues. Although this strategy has been adopted in a number of studies, active targeting is limited by the need for nanoparticles to be in close proximity to the targeted tissue.[11] Although targeting might increase selectivity and cell uptake *in vitro*, effective targeting *in vivo* is minimal. It is necessary to consider the broader role of particle morphology when translating nanoparticles *in vivo*; for example, active targeting motifs can increase properties such as particle size, significantly changing the distribution behavior and cellular uptake.[12] With this in mind, adapting the morphology of nanoparticles to synergistically enhance efficacy is an important strategy. For example, elongated particles show deeper tumor tissue penetration and interact with a larger volume fraction of the surrounding vasculature than that of spherical particles.[13] With shape and size being such essential factors that influence targeting properties, the versatility of polymeric vesicles can be effectively utilized to engineer materials that can be adaptive to their direct environment.

Adaptive nanosystems, which display unique morphological features in order to synergistically enhance performance *in vivo*, can be effectively engineered utilizing the self-assembly of block copolymers (BCPs). The capacity of synthetic BCP vesicles ('polymersomes') to embody a number of key properties such as compartmentalization and discretization have been established.[14–16] BCP membranes display the same amphiphilic character as lipids but are more stable and chemically versatile.[17] Self-assembly of BCP nanosystems has been studied extensively to unravel their dynamics, with polymer geometry and packing determining particle morphology (*e.g.*, lamellar, micellar or vesicular; Figure 3).[18] Although micellar systems show great promise as drug delivery platforms, their relative instability compared to polymeric vesicles is disadvantageous for long circulation and targeting studies. The chemical versatility of polymersomes allows the engineering of various morphologies with control over chemical composition, size, shape, surface chemistry and functionality being of significance when their performance in biological context is to be considered and evaluated.

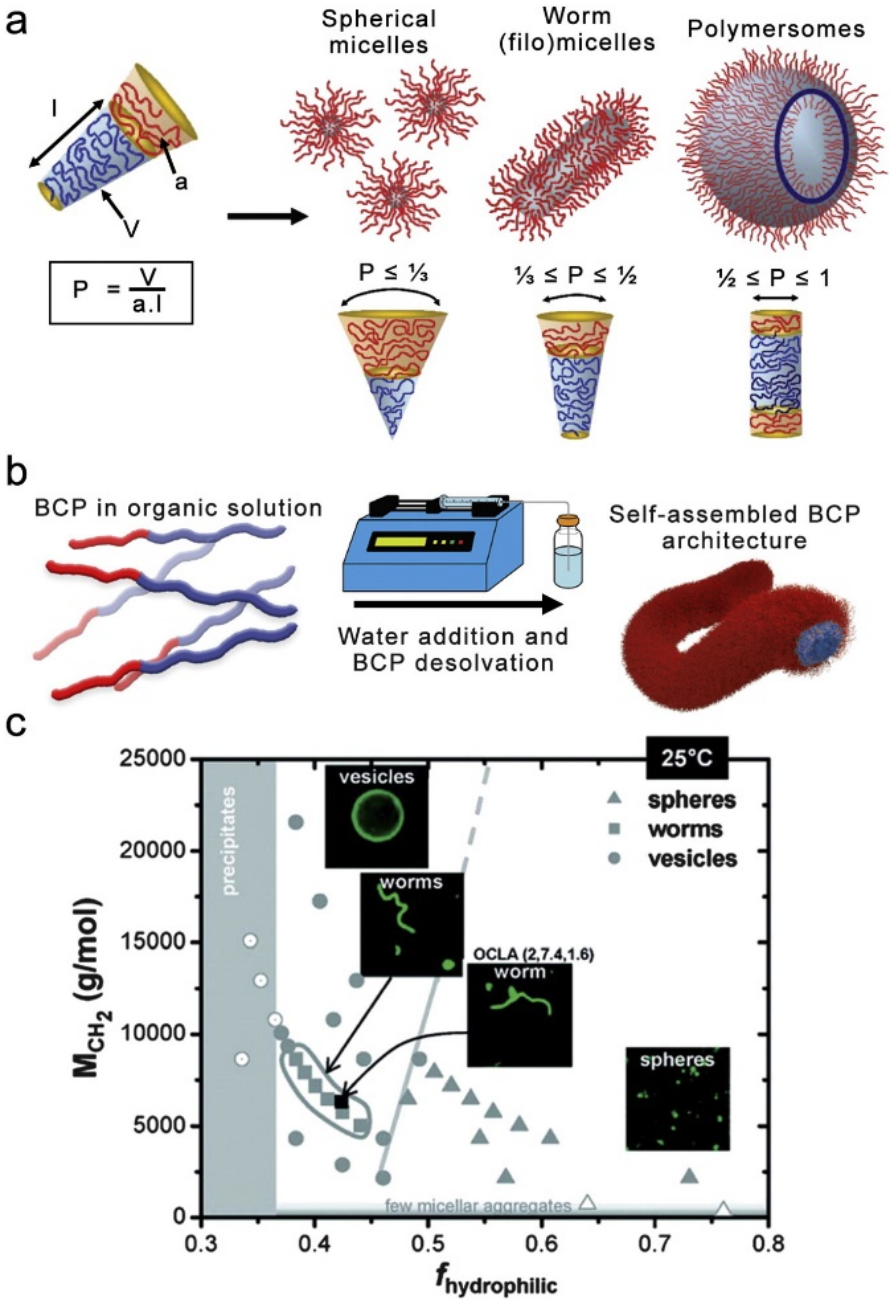

Figure 3. Schematic demonstrating the bottom-up design of the controlled self-assembly of block copolymers into nanoparticles, where intelligent polymer design (a) and self-assembly conditions (b) can influence resulting particle morphology (c). Reprinted with permission.[1]

2. Block copolymer particles as platforms for therapeutic and smart drug delivery applications

2.1 Polymeric nanoparticles as therapeutic platforms

There is a wide range of copolymers and fabrication methodologies that have been presented in the literature, many of which have properties that have potential for nanomedical applications.[1] Of particular interest is the ability to adapt spherical polymersomes into other morphologies (such as tubes, discs and stomatocytes) using shape transformation methodologies, which greatly enhances the

versatility and the applicability. Although there has been substantial progress towards the generation of polymersomes for biological applications, this is usually accomplished *via* the self-assembly of nonbiocompatible/degradable components comprising building blocks such as polystyrene (PS) and poly(dimethyl siloxane) (PDMS).[19,20] To further develop the utility of copolymers, an important consideration is biocompatibility, which can be imparted through the use of biodegradable subunits such as polyesters and polycarbonates. With this in mind, biodegradable polymers, such as poly(ε-caprolactone), polylactide and poly(trimethylene carbonate), have been presented as excellent candidates for developing nanostructures that are inherently biocompatible; however, achieving control over the self-assembly of such materials remains a challenge. Fine-tuning the self-assembly of particular copolymers can be accomplished through systematically engineering both physical and chemical aspects. Poly(ethylene glycol)-*block*-poly(ε-caprolactone) (PEG-*b*-PCL) has been extensively studied and is FDA-approved for biological applications. PCL undergoes degradation by means of enzymatic and nonenzymatic hydrolysis into nontoxic products and has been shown to undergo self-assembly using the biocompatible direct hydration method, which has potential for the encapsulation of active materials.[21] Investment in this kind of nanoengineering can fuel the development of functional nanosystems by providing insight and expertise in the fabrication of copolymeric nanoparticles with well-defined morphological characteristics, which is of great significance to a broad scientific audience.

Another important feature of polymersomes that has an impact over their implementation in biomedical applications regards the permeability of their membrane. A number of different approaches have been described to provide control over the permeability of copolymeric bilayers. For example, polyionic complex-based polymersomes (PICsomes) have been shown to be permeable to small compounds due to the loose packing of their membranes.[22,23] Engineering the composition of the polymersomal membrane can be used to introduce hydrolysis, pH- or UV-sensitive moieties that can induce stimulus-responsiveness permeability.[24,18,19] The porosity of polymersomes has also been established by the insertion of channel proteins, such as OmpF or Aquaporin Z, creating channels for selective molecular transportation.[25] Recently, polymersomal nanoreactors have been developed that encapsulate enzymatic cargo, which are capable of regulating cascade reactions and can be applied in cellular therapies as a kind of ‘synthetic organelle’. These synthetic organelles are interesting candidates as to not only gain a deeper understanding of the intracellular processes but also to enhance the activity of existing organelles and actively produce drugs.[25]

2.2 Adaptive polymeric nanoparticles for smart drug delivery

Having established the design principles that underpin polymersome fabrication and control over morphology,[26,18] it is also pertinent to consider how we might induce more dynamic adaptability into such systems. Such a paradigm shift from exploring the fundamental principles of polymer self-assembly towards the design of dynamic systems has significant potential in the generation of smart

drug delivery technologies. Smart polymeric technologies are capable of undergoing some kind of morphological switch in response to a change in the local environment as a consequence of a chemical or physical stimulus. For example, stimulus-responsive polymersomes have been designed to respond to certain biological environments in order to allow site-specific, 'on-demand' release of cargo (Figure 4).[27]

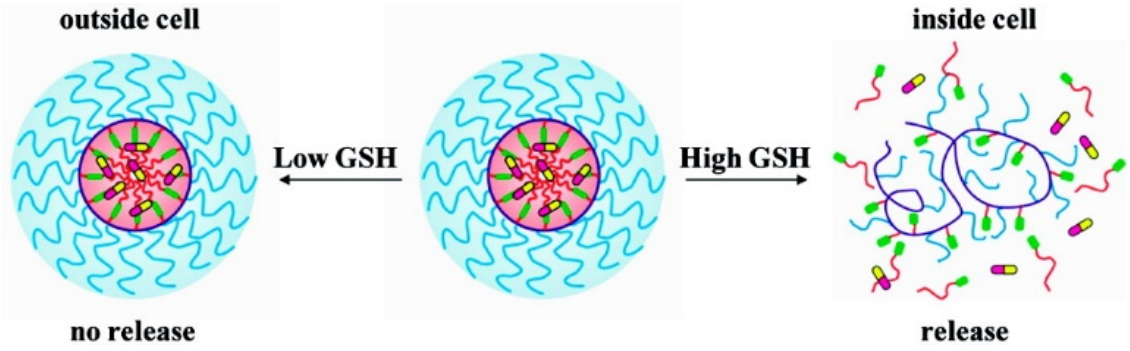

Figure 4. Schematic showing the responsive behavior of a redox-responsive nanoparticle influenced by the concentration of glutathione (GSH) corresponding to the environment inside and outside of cells. Reprinted with permission.[28]

Size switchable nanoparticles (SSNs) have been developed to adjust their size when triggered by an environmental (internal) or external trigger. [29–31] Chemically, SSNs respond to changes in local environment, for example, in peripheral tumor tissues through bond cleavage, protonation, or conformational changes that effect major changes in the overall structure. For application in treatment of solid tumors, SSNs are engineered to adapt their hydrophilic/hydrophobic properties, association/disassociation interactions, or alter their surface charge in response to increased local acidity (pH 6.5–6.8), which enables them to preferably embed and thereby improve therapeutic outcomes. In comparison with conventional stealth nanoparticles, SSNs can achieve adaptive behavior so that a morphological transformation occurs after accumulation/retention in the tumor region, resulting in the generation of smaller nanoparticles (< 50 nm).[32] The resultant smaller nanoparticles can undergo deeper tumor penetration and efficient nuclear uptake, whereas the original larger particles display a prolonged circulation time, all of which is integrated into a single nanoplatform. Alternative triggers, such as enzyme-, pH- and reduction/oxidation-responsive materials have also been fabricated to induce cargo release around tumor tissue.[33] External stimuli, such as temperature, light or ultrasound are additional intriguing features for intelligent polymer drug delivery platforms with increased efficacy and efficiency.[34] Wang *et al* developed ultra-pH-sensitive cluster nanobombs (SCNs) by rational self-assembly of poly(ethylene glycol)-b-poly(2-azepane ethyl methacrylate)-modified PAMAM dendrimers (PEG-b-PAEMA-PAMAM/Pt), in which a platinum prodrug was conjugated.[29] After accumulation/retention in the acidic tumor region, the PAEMA block became hydrophilic due to its ultrasensitive pH responsiveness and rapid protonation, resulting in cluster

disassembly and instantaneous disintegration of the superstructure into small nanoparticles. Upon disassembly, covalently conjugated Pt-prodrug on the dendrimer was specifically reduced by intracellular abundant GSH to great therapeutic effect. Matrix metalloproteinases (MMPs), especially MMP2, are recognized to be involved and overexpressed in many stages of human cancers.[35] Nanoparticle delivery systems bearing MMP-sensitive moieties allow specific stimulus responsiveness in the tumor region. A sophisticated design of size changeable nanocarriers based on the abnormal expression of MMP-2 in the tumor region was recognized as a promising approach for dual-targeted delivery to solid tumors. In a recent study, an SCN with tunable size was prepared by Hu *et al*, which was formed by covalent conjugation of hypoxic microenvironment targeting tungsten oxide nanoparticles (~5 nm) with a matrix MMP-2 cleavable peptide (Pro-Leu-Gly-Val-Arg-Gly).[35] Upon entering into the MMP-2 overexpressed tumor region, bond cleavage resulted in detonation of the nanobomb, effectively releasing tungsten oxide nanoparticles to achieve deep tumor penetration. A switchable spiropyran-based nanoparticle that responds to an exogenous trigger (UV light) has been described by Kohane *et al*,[36] which upon UV light irradiation underwent a volume decrease, enhancing tissue penetration and drug release. Although nanoparticle characteristics such as size, chemical composition and membrane permeability are critical decisive factors in their performance in drug delivery applications, the effect of shape remains elusive. However, one can envision that the morphological characteristics of nanoparticles might have an influence on their capacity for drug transportation and release. It is important to explore the behavior of a wide range of shapes of nanoparticles in order to understand and develop system versatility and utility.

Micro or nanoreactors are versatile systems that allow for catalytic or cascade reactions to take place in a controlled environment such as the inner compartment of polymeric vesicles. Driven by membrane permeability, nanoreactors can process active compounds using catalysts sequestered inside the vesicle, releasing products in the vicinity of the particle.[37,38] Such compartmentalized systems reduce the diluting effect that occurs when free active compounds are distributed in the body and prevents premature chemical degradation or processing by the immune system. Inspired by viruses, several types of nanoreactors have been developed. Responsive nanoreactors are highly interesting candidates as they rely on site-specific activation of the catalytic properties of the system. The *in situ* activation of drugs, or prodrugs, can occur by deactivating the active compound by, for example, immobilization on the polymer shell.[39] In a specific example, the anticancer drug camptothecin (CPT) was immobilized in the membrane of a pH-sensitive polymersome (Figure 5) via an oxidation-sensitive linkage. Glucose oxidase, a highly efficient catalyst generating H_2O_2 through oxidation of glucose and often studied as an oxidation therapeutic, was encapsulated in the vesicle. By lowering the pH, the membrane permeability was increased allowing glucose to be converted by the enzyme into gluconolactone and H_2O_2. The production of the latter increased oxidative stress in tumors, inducing cell death, and additionally released the CPT into the environment.

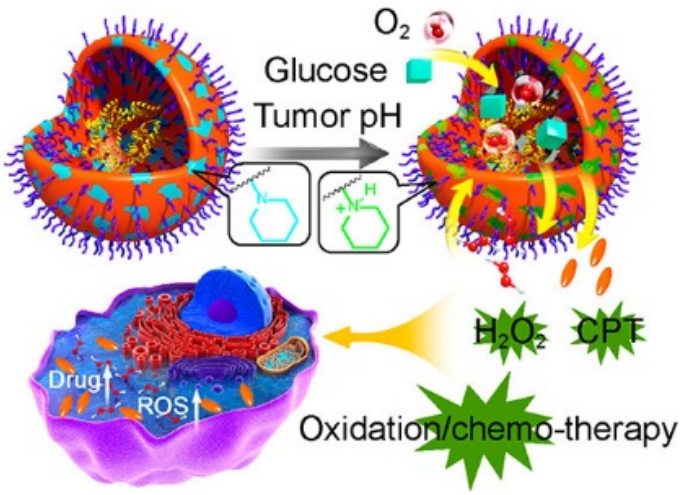

Figure 5. Prodrug-based nanoreactor displaying increased permeability in low tumor environmental pH, thus activating the release of CPT and the formation of peroxide. Reprinted with permission.[39]

Although our ability of decorating structures and creating certain functions to mimic the natural environment has improved greatly over the years, it also has led to the development of multifunctional nanoparticles that tend to suffer from over-complexity. Each addition influences not only the materials' physicochemical properties but also, and more importantly, their biological behavior. Although this over-complexation might aid in the understanding and development of complex materials such as artificial cells and organelles, it is vital for the progress of this research field to maintain focus on the subject and, described by 'less-is-more', steer clear from researching materials that in the end do not benefit the purpose. Additionally, as functionalization on a high number of particles, as is usually the case, causes a statistical disparity in added functionality to particles, more additions lead to larger significant difference between the particles. This broad deviation in true functionality might result in unwanted or unrealistic effects when studying the biological response of these particles. The morphology of nanoparticles, including size and shape, is an interesting factor to study how different particles migrate through the body and penetrate tissue and cells. Demonstrated in multiple studies, the morphology has such a profound effect on these subjects that the addition of multiple functionalities might prove redundant.

3. Controlling the morphology of polymeric nanoparticles

Pioneering research was performed by the Mitragotri group on the fabrication of nanoparticles with different morphologies.[40,41] This was achieved using a polymer substrate which was subsequently subjected to stretching, yielding elongated particulates of different sizes and aspect ratios. The effect of particle morphology on uptake in macrophages or tumor cells along with biodistribution was studied. Elongated or wormlike structures were found to inhibit phagocytosis by macrophages due to their high aspect ratio and high flexibility.[42] On average, nanoparticles with higher aspect ratios inhibited uptake more extensively compared to spherical particles. Aside from

elongated structures, several, more exotic, morphologies were studied regarding cell uptake, internalization and biodistribution. The DeSimone group developed the PRINT technique, in which a liquid polymer precursor can be molded and cured to form any desired shape, finding that particle design influences cellular integration pathways and cell uptake.[43,44] Although present methods provide sturdy and monodisperse particles, their solid nature and large size introduce limitations in drug encapsulation and subsequent utilization in nanomedicine.[45] Using a different approach, the Lecommandoux group investigated the effect of hypo- and hypertonic shock upon the morphology of polymersomes and observed the formation of nested vesicles and stomatocytes under hypertonic conditions.[20] Over the past decade, the van Hest group has been developing methodologies to control shape transformations of polymersomes, with effective methodologies developed for both PEG-poly(styrene) (PEG-PS) and PEG-poly(D,L-lactide) (PDLLA).[47,48] Significantly, shape transformations of spherical PEG-PDLLA polymersomes into both oblate and prolate structures can be induced by an osmotic pressure applied on the membrane during low-temperature dialysis. Physical factors such as polymer composition and membrane thickness were found to influence the subsequent direction of shape transformation that may additionally influence membrane flexibility and stiffness. Oblate structures, also named stomatocytes, consist of a stomach which has an opening connecting the outer environment to the inner lumen. Such stomatocytes have been utilized in the fabrication of nanomotors towards biomedical applications.[48,49] Driven by platinum nanoparticles, stomatocyte nanomotors were a significant development in the generation of autonomous, chemotactic nanotechnologies with propulsion generated by degradation of H_2O_2 into oxygen.[50] Abdelmohsen *et al* demonstrated that enzymatic cascade reactions inside stomatocytes could be utilized as a form of biocompatible propulsion, being induced by the presence of both catalase and glucose oxidase (Figure 6).[51] Catalase is capable of efficiently decomposing hydrogen peroxide into water and oxygen. When combined with glucose oxidase, glucose can be decomposed into hydrogen peroxide, which is then decomposed by catalase into oxygen nanobubbles. The generation of oxygen results drives the thrust of these stomatocytes.

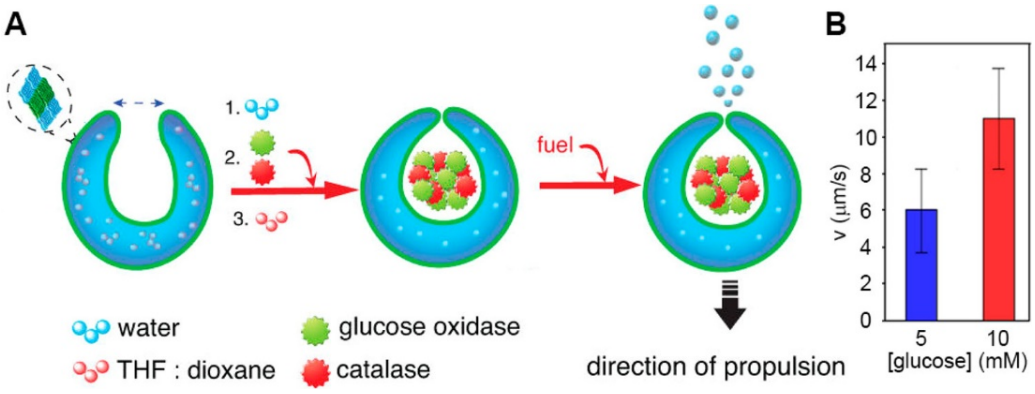

Figure 6. Enzyme-loaded stomatocytes generate oxygen by fueling catalase with glucose via a cascade reaction yielding self-propelling particles (A). The concentration glucose influences the particles' speed (B). Reprinted with permission from reference.[52]

Incorporating active macromolecules into stomatosomal compartments is an interesting basis for their implementation for nanomedical applications such as drug delivery and immunology. However, the nondegradable nature of PS-based nanocompartments, severely limits their applications in biological settings. To this end, van Hest *et al* explored the utility of biodegradable copolymers for self-assembly to unravel their potential in nanomedical research (Figure 7).[47] With fine tuning of the self-assembly through systematic engineering of the physical and chemical process, elongated nanotubes and bowl-shaped stomatocytes were prepared from biodegradable subunits. The ability to design such structures from biodegradable components holds great potential for nanomedical applications.[53]

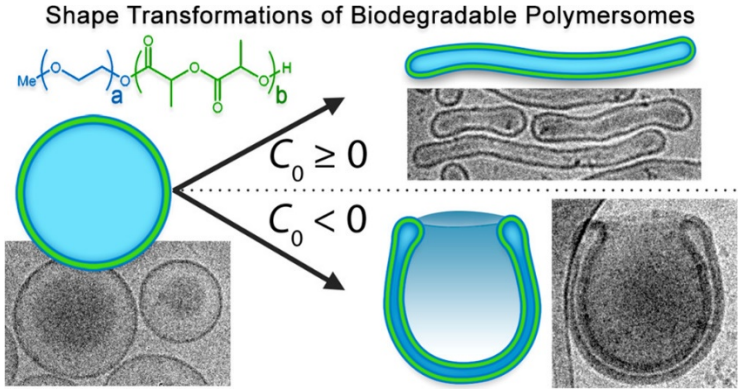

Figure 7. Schematic describing the influence of the spontaneous curvature on the resulting morphology of osmotically induced shape-transformation on PEG-PDLLA polymersomes. Reprinted with permission.[47]

4. Influence of shapes of nanoparticles on their anticancer effects *in vitro*

As has been alluded to, the morphology of nanoparticles plays a large role when their interactions with cells and organs have to be considered. The ability to engineer polymeric nanoparticles with such interesting morphological characteristics and the capacity to be adapted for, or in response to, specific biological environments is now being harnessed for proof-of-concept biochemical testing both *in vitro* and *in vivo*. Invaluable studies were performed to compare the antitumor efficacy of nonspherical nanoparticles to their spherical counterparts *in vitro* and *in vivo*. A delicate interplay of factors concerning cellular uptake mechanisms, distribution, and tumor accumulation leads to the notion that the morphology of nanoparticles seemingly affects the biodistribution and the reduction of tumor volume. Dendrimeric structures combined with docetaxel were able to form either nanospheres or nanosheets by varying their molecular weight ratios. The antitumor efficacy *in* vivo was almost 2-fold better for the sheets than that of the spherical particles.[54] Discoidal porous silica nanoparticles demonstrated a five-fold increased accumulation in breast tumor mass.[55] Formation of PLGA nanoparticles demonstrating porous matrix and rough surface showed increased *in vivo* antitumor efficacy compared to nonporous, smooth PLGA particles, owing to their

high drug loading and high dispersion in tumor sites.[56] Until now, systematic studies have only been performed with elongated particles, in particular rod-like filomicelles, which will therefore be the main topic of discussion in the next sections.

4.1 Cellular internalization of shaped micelles

A typical approach to improve or induce cellular uptake of nanoparticles is to trigger the energy-dependent cell endocytosis mechanisms to undergo clarthrin- and caveolae-mediated endocytosis or micropinocytosis.[57] The mechanism of endocytosis is not only dependent on the nature of the targeted receptors and cell types but also on the particles' physicochemical properties, such as size, surface chemistry, shape, and elasticity.[58–61] For the effect of morphology, it seemed that the local geometry, local curvature and mean curvature, of particles in contact with the cell affect the endocytosis efficiency.[62,63] Park *et al* fabricated keyboard character shapes and found that those with sharp features and higher aspect ratios (such as letter I, number 1, and arrow key) adhere more to the LnCAP prostate cancer cells and are internalized within 75 min. In contrast, shapes without sharp features, such as the letters D, G, O, and the number 0, were unable to attach or penetrate the cells.[64] The sharper objects seemed to unable the cells to recruit more actin filaments and attach and engulf the objects than those without sharp features. Ma reported that PEGylated graphene nanosheets could hardly be internalized, and more likely adsorb onto or partially insert into the cell membrane in face-on/edge-on configurations.[65] Cylindrical polystyrene nanoparticles showed increased specificity of endothelial targeting compared to the spheres,[66] due to the balance of polyvalent interactions that favor adhesion and entropic losses as well as shear-induced detachment that reduce binding.

For cylindrical particles, the aspect ratio showed great influence on the cell uptake behavior. Shapes with higher aspect ratios could be internalized by the cells faster than those of lower aspect ratios,[44] which might be due to their larger surface area that enhances the interaction with cell membranes. However, contradictory results have been reported. For other nanoparticles, high aspect ratios seemed to reduce internalization and prolong the blood circulation time and cell targeting capability.[66,67] For nanoparticles shaped as the keyboard character solid arrow, internalization involved first the attachment of the arrowhead part to the cell membrane for 50 min and cell membrane extension to induce internalization, followed by reorganization of actin to allow uptake of the remainder of the nanoparticle. The internalization happened within approximately 80 min and was completed after 2-3 h.[64] Stenzel *et al* reported that fructose-based cylindrical micelles with smaller aspect ratios were internalized by cells significantly more and faster than medium and long ones by breast cancer cells in 2D and 3D tumor spheroids models.[68] Most likely, long rods need to overcome a higher membrane bending energy barrier during endocytosis than short ones. Discher *et al* investigated systematically the endocytosis of filomicelles of PEG-PCL and PEG-poly(butadiene) (PEG-PBD) by phagocytic cells and nonphagocytic cells. It was found that shorter micelles were taken

up more than the long ones (3 μm) by phagocytic cells and multisite attachment between cells and filomicelles was observed (Figure 8A).[67] Under flow conditions, short filomicelles adhered to and were taken up significantly more by phagocytes owing to the stronger interaction with the cells and a lesser effect of the flow; shear forces tend to minimize the interactions of long filomicelles with phagocytes, as they flow-align them and pull them off phagocytes as they come into contact. Fragments of long filomicelles might break off faster than the shorter ones and only micelles smaller than 2.5 μm were taken up significantly by the phagocytes (Figure 8B), while nonphagocytic epithelial cells rapidly pinocytosed filomicelles and trafficked them actively to the perinuclear region. The pinocytosis process reduced the length of the filomicelles and left only 2.5-μm long micelles in the culture (Figure 8C).

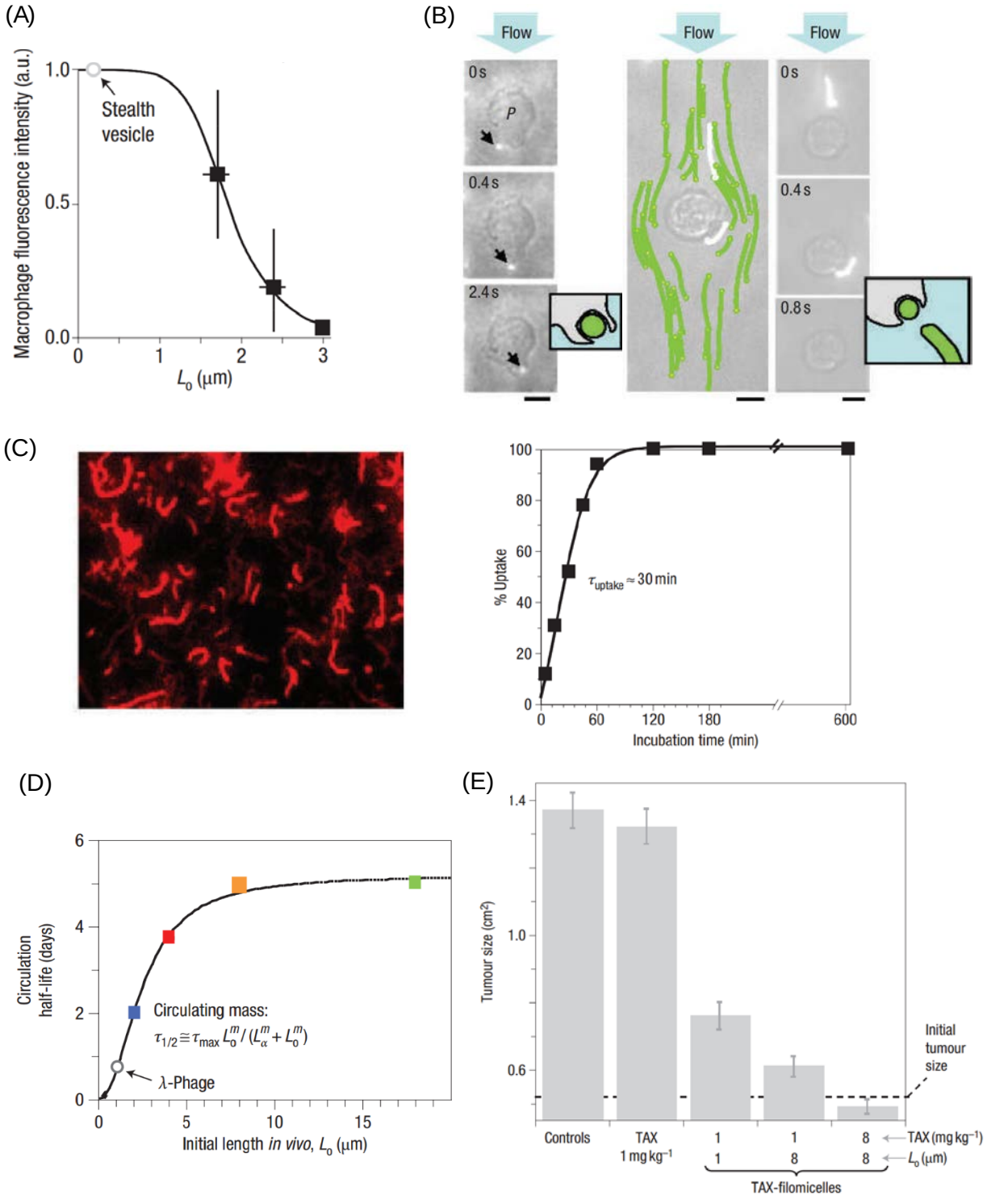

Figure 8. *In vitro* and *in vivo* experiments with filomicelles. (A) Fluorescence intensity of macrophages incubated with fluorescent filomicelles of varying length for 24 h in static cultures. (B) In an *in vitro* flow chamber with immobilized phagocytes, long filomicelles (right) flowed past the cells and left a fragment. Smaller micelles were captured (left). Scale bars represent 5 μm. (C) Uptake of filomicelles by epithelial cells. (D) Circulation half-life of filomicelles as a function of micelle length. (E) Shrinkage of A549 tumor xenografts in nude mice which were injected i.v. with PTX loaded filomicelles containing different PTX doses (n = 4). Reprinted with permission.[67]

For cylindrical particles, anchoring active targeting ligands not only changes the surface properties but also potentially changes the way of cell entry.[69] Based on the long circulation and minimal accumulation of filomicelles in the rat lung,[70] the development of specific targeting cylindrical particles to specific sites can eventually lead to effective drug delivery.[66] Discher *et al* designed antibody coupled filomicelles with tailored receptor ligands of high and low affinity to manipulate the specific targeting to endothelial walls.[71] The biotinylated wormlike micelles were internalized by receptor-mediated endocytosis either through packaging of the micelle or fragmentation.[72] The fructose moieties on the cylindrical micelle surfaces promoted their internalization via receptor-mediated endocytosis owing to the excellent affinity of fructose to GLUT5 receptors that are overexpressed on breast cancer cells.[68]

Moreover, the chemistry of the materials influences the cell uptake as well. PEG-PCL modified with aromatic moieties in the hydrophobic domain, PEG-poly(alpha-benzyl carboxylate ε-caprolactone) (PEG-PBCL), assembled into filomicelles that maintained flexibility, but showed an increased filomicelle yield (93% vs 79%). The cell entry of PEG-PBCL filomicelles by A549 cells increased with first-order kinetics (time constant of 85 h) compared to a parabolic curve of PEG-PCL filomicelles.[73] PEG-PCL filomicelles had higher accumulation initially but were surpassed by PEG-PBCL on day 3, suggesting that the cell uptake was dominant in the cell delivery compared to the drug release, for which the PEG-PBCL system was slower. Antibody coupled nanorods showed higher adhesion propensity than spherical particles that carried the same antibody and several folds higher adhesion than the nonspecific antibody coupled nanorods in static conditions and under flow.[66] The above results suggest the necessity to evaluate the contribution of shape towards internalization in the context of surface chemistry, material stiffness and concentration.[45,69,74–77]

4.2 Cellular internalization of shaped polymersomes

Compared to wormlike micelles, tubular nanoparticles can encapsulate and deliver water-soluble substances within their lumen and hydrophobic molecules within their membrane.[18,78] As a typical tubular morphology, carbon nanotubes are held together by strong covalent bonds, which makes them stiff and inflexible, and their entry into cells occurs through a “needle-like” penetration of the membrane.[79,80] They were cleared from the body within hours after intravenous injection.[81] Only recently, soft polymeric tubular polymersomes were devised based on a variety of methods. However, there have only been very limited reports on the internalization of polymersome tubes. Battaglia *et al* reported the effects of polymersome shape on internalization kinetics of pH-sensitive poly(2-(methacryloyloxy)ethyl phosphorylcholine)-poly(2-(diisopropylamino)ethyl methacrylate) (PMPC-PDPA) tubular polymersomes.[82] The spherical polymersomes were previously applied as carriers for drugs and DNA delivery.[83,84] Kinetic studies revealed a biphasic uptake profile of tubular polymersomes by neutrophils, corresponding to an initial quick binding step before 9 h followed by a

slow internalization after 9 h (Figure 9). In comparison, the spherical polymersomes showed a rapid internalization followed by a single plateau.[82] Despite the unfavorable tube length for endocytosis, the tubes displayed high cellular uptake. This was ascribed to the multiple binding sites of PMPC for its receptors, leading to local destabilization and deformation of the plasma membrane, and progression to full endocytosis with the assistance of components of the cytoskeleton and other molecular endocytic players. The quick internalization rate, higher drug loading and similar uptake number of these tubes compared to spherical ones highlight their higher drug delivery capacity. These tubes loaded with drugs displayed increased cellular ATP levels of parkin mutant fibroblasts, thus rescuing mitochondrial function without any apparent cytotoxicity.[85]

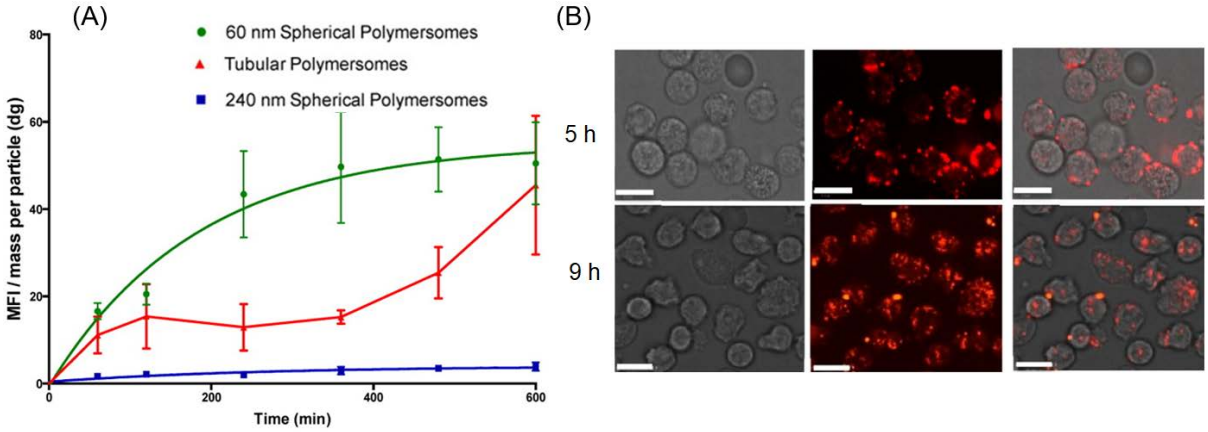

Figure 9. Internalization of tubular polymersomes. (A) The uptake rate of rhodamine-conjugated tubular polymersomes in neutrophils measured by flow cytometry. (B) Binding and internalization of tubular polymersomes in neutrophils visualized by confocal microscopy at 5 and 9 h. Scale bar represents 5 μm. Reprinted with permission.[82]

Huang *et al* investigated the interaction between the tubes and the cell membrane using a Dissipative Particle Dynamics (DPD) simulation method.[86] Three different interaction pathways were identified: membrane wrapping, tube-membrane fusion and tube pearling, depending on the tube-cell membrane adhesion strength and membrane surface tension. A strong tube-cell membrane adhesion induced significant membrane wrapping. Soft tubes can be wrapped from the top by membranes via membrane monolayer protrusion, which together with tube deformation cooperatively makes the wrapping dynamics heterogeneous along the axial direction. A weak tube-cell membrane adhesion promoted tube pearling. The tubes can sometimes fuse with cell membranes under highly positive membrane tension, and molecules diffuse from tubes to membranes, which leads to the increase of tube tension and promotes tube pearling.

4.3. Influence of shape on cytotoxicity

Cytotoxicity is the direct and cooperative result of the internalization and drug release from the shaped particles. The cylindrical nanoparticles have a large volume for drug loading and multiple

and strong binding to the cell membrane and are expected to lead to highly efficient killing of target cells. The loading capacity, retention, and release of the drugs are important factors. Generally, drug loading capacity of filomicelles depends on the interaction between drug molecules and the copolymers.[73,87,88] The filomicelles of PEO-PCL (5-6.5 kDa) could load paclitaxel (PTX) of approximately 2.8 wt.%, twice as much as their spherical micelles. *In vitro* PTX release rates from both morphologies were similar, and were faster at pH 6.8 (mimicking the slightly acidic cancerous tissue environment) than at pH 7.4 (normal tissue pH). These results are contradictory to a previous report that shows a higher release rate from rod than spheres.[89] The PEG-PBCL filomicelles showed enhanced PTX loading by 40% and decreased PTX leakage compared to PEO-PCL filomicelles.[73] MTT assay results indicated that PTX-loaded PEG-PBD and PEG-PCL filomicelles showed 5-fold greater anticancer activity against A549 human lung cancer cells than that of free PTX.[33]. PTX-loaded PEG-PBCL filomicelles further increased cytotoxicity 2.5-times compared to PEG-PCL filomicelles, and resulted in the greatest aneuploidy among surviving cells compared with PEG-PCL filomicelles and free PTX. The increased hydrophobicity of PBCL improved the PEG-PBCL filomicelle cellular uptake compared to PEG-PCL, despite of the slower drug release kinetics. It is noted that the empty filomicelles of PEG-PCL and PEG-PBCL were far less toxic than the clinically used Cremophor/EL in TAXOL.[73,90] The IC_{50} of DOX-loaded folate-targeted cylindrical micelles based on cyclodextrin was half of the nontargeted micelles and free DOX using KG-1 (folate positive receptor) cell lines, illustrating that targeting ligands can further enhance the cell internalization and cytotoxicity of cylindrical nanoparticles.[87]

5. Effect of shape on the performances of nanoparticles *in vivo*

Considering the great potential of cylindrical particles as drug carrier, *in vivo* evaluations of shaped particles with regard to blood circulation, biodistribution and tumor inhibition were conducted.[66,67,71,73,91] To prevent premature drug release caused by insufficient *in vivo* stability and low drug efficacy owing to low intracellular drug concentration that polymeric nanomedicines normally encounter,[92,93] chemical crosslinking, tumor specific targeting as well as stimulus-sensitive cylindrical nanoparticles were developed.[66,68,91,94] The promising application of cylindrical nanoparticles in drug delivery systems was thus demonstrated.

5.1. Circulation time

Discher's pioneering work [67,90] demonstrated that the soft PEO-PCL filomicelles could circulate up to one week after intravenous injection in rats, which was about ten times longer than any known synthetic spherical nanoparticles. Biodegradable rod-like micelles (40 nm in diameter and 600 nm in length) possess a minimal uptake by the RES and a longer blood circulation half-life ($t_{1/2\beta}$ = 24.23 h) than that of spheres ($t_{1/2\beta}$ = 8.39 h) in mice.[95] Generally, spherical nanovehicles can enter cells and circulate *in vivo* for a few hours, while spherical microparticles are cleared instantly in the

microvasculature of organs and do not enter most cells. Notably, the flexibility of PEG-PCL micelles are about ten times lower than PEG-PBD micelles; however, they both could circulate for more than a week, indicating that the flexibility of filomicelles was important but weak in its effects *in vivo*.[67] Nevertheless, the circulation time was dependent on the length of filomicelles, and PTX loaded filomicelles with length of approximately 8 μm had the longest circulation time compared to spheres and other filomicelles (Figure 8D).[67] Since clinical studies have demonstrated that circulation times of spherical carriers are generally extended threefold in humans over rats,[96] the circulation time for filomorphologies could approach one month in humans. Such long circulation times may offer high drug efficacy against cancer cells by favoring drug accumulation through the leaky vasculature of solid tumors [77,97,98] and reduce off-target effects.[99]

5.2. Biodistribution

The MPS system of the liver and spleen is responsible for filtration and clearance of circulating particulates and some filamentous viruses. The biodistribution study of PEG-PCL filomicelles in rat organs showed that the liver and, to a lesser extent, the spleen dominate the (slow) clearance of filomicelles.[67] They had measurable accumulation in the kidney, owing to hydrolytic degradation products that might permeate the fine mesh of the kidneys. Moreover, the PEG-PCL filomicelle had moderate buildup in the lung, which was consistent with the minimal lung accumulation of poly(2-ethyl-2-oxazoline)-PCL-based filomicelles in rat.[70] Coupling antibodies changed the biodistribution of the cylindrical nanoparticles *in vivo*. In healthy mice, specific cylindrical nanoparticles, surface-modified with anti-intracellular adhesion molecule 1 or antitransferrin receptor antibodies, exhibited much higher lung or brain tissue accumulation, respectively, than spheres with the same surface chemistry and IgG-coated cylindrical nanoparticles.[66] Stenzel *et al* studied cylindrical micelles' biodistribution in mice as a function of crosslinking and folate conjugation of micelles, which were based on a block copolymer of polyethylene glycol methyl ether acrylate and oxoplatin conjugated acrylic acid.[91] The crosslinked micelles displayed an increased drug accumulation in the organs compared to noncrosslinked ones. The targeting worm micelles had 3- or 7-fold higher accumulation in organs (especially spleen, liver and kidneys) than spherical micelles with or without folate, respectively. The long residence time on the cell surface before internalization for cylindrical particles[82] and the polyvalent interactions between targeting ligands and receptors on the cell surface[66] contribute significantly to tumor accumulation and penetration.

5.3 *In vivo* antitumor efficacy

The first antitumor study of filomorphologies was done using PTX-loaded PEG-PCL filomicelles of 1 μm or 8 μm in length. At a dosage of 1 or 8 mg PTX/kg, the filomicelles were injected i.v. into A549 tumor xenografts in nude mice. The 8 μm filomicelles, having the longest

circulation time, demonstrated the greatest tumor shrinkage in mice compared to spheres and other filomicelles due to the effective delivery of PTX into tumor cells. Notably, 8 μm long filomicelles at 1 mg PTX/kg brought about the same therapeutic effects as 1 μm long filomicelles at 8 mg PTX/kg (Figure 1E).[67] Both increase in micelle length or PTX content resulted in a doubling of apoptosis of cancer cells in the tumor and a similar extent of decrease in tumor size. Apparently, the circulation time and drug loading content as well as concentration of filomicelles *in vivo* all affect their final therapeutic performance, providing a clear indication to lung tumors. Preliminary *in vivo* antitumor experiments in nude mice bearing A549 xenografts showed that PTX-loaded PEG-PBCL filomicelles produced 25% tumor shrinkage in 2 weeks at one-fourth PTX dosage of PTX-loaded PEG-PCL filomicelles.[73] The high potency of PTX-loaded PEG-PBCL filomicelles towards the same tumor indicates that simple chemical variation may contribute to high antitumor efficacy. The high aspect ratio in rod-shape nanoparticles affects their interaction with cancer cells and has a great potential to promote their tumor penetration depth, which innovates the approach in nanomedicine design. For instance, compared with nanospheres with the same hydrodynamic diameter, quantum dot-based nanorods displayed enhanced penetration in orthotopic mammary tumors at 1 h postinjection in mice.[13] Additionally, single-walled carbon nanotubes displayed enhanced tumor penetration compared with spherical quantum dots in U87MG tumor models.[100] The activatable porphyrin nanodiscs (10 to 30 nm) in an *in vitro* model showed 5-fold enhanced diffusive properties in a collagen-rich environment, demonstrating the potential improvement in penetration in dense solid tumors. [101]

Stimulus-responsive cylindrical nanoparticles can facilitate the site-specific destabilization and fast drug release in the diseased sites in response to special cues in the tumor environment, providing benefits for further accumulation inside tumor cells. For instance, tumor tissue pH responsive worm micelles (PHWMs) loaded with photosensitizing drug chlorin e6 (Ce6)[94] displayed higher cellular uptake, increased singlet oxygen generation and improved photoactivity when KB cells were treated at pH 6.8–6.0 upon light illumination compared to pH 7.4. Moreover, treatment of KB tumor bearing nude mice with a single dose of Ce6-loaded PHWMs showed more accumulation at the tumor site than nonsensitive micelles or free Ce6, leading to 5.2 time higher tumor growth inhibition than those treated with free Ce6.

6. Conclusion

The past decade has witnessed increasing interest in the development of morphologically discrete nanoparticles, in particular polymersomes and micelles, as advanced carriers for anticancer nanomedicines. The novel fabrication methods developed by different research groups make it possible to prepare sophisticated polymersomes and micelles with varying morphologies ranging from

wormlike micelles and tubes to discs and stomatocytes. It is interesting to note that shaped nanoparticles and nanomedicines show distinct behaviors from spherical ones *in vitro* and *in vivo*, which signifies the important role of vehicle morphology in cancer therapy. Gaining control over particle morphology is an ever-increasing field of research that will hold a solid future in nanomedicine applications. However, there remain many pitfalls to be overcome or be taken into consideration on conducting follow-up research or translating this knowledge into clinical trials. One of the pitfalls of designing different morphologies for drug delivery platforms is that although our knowledge of the effect of morphology *in vivo* and *in vitro* is ever increasing, cell interactions and *in vivo* processes such as opsonization can remain extremely shape or size specific. This indicates that utilizing the morphology, size or shape of drug delivery platforms might increase the specificity but decrease general applicability.

In spite of significant progress, fabrication of polymersomes and micelles with shaped morphologies remains empirical. So far, wormlike micelles, tubes, discs and stomatocytes can be prepared only from certain copolymer at a narrow composition range and under particular conditions. In most cases, employed polymers are not biodegradable or biocompatible, which renders previously reported shaped nanoparticles with little potential for clinical translation, although they can be interesting as a model to study the effect of shape on drug delivery *in vitro* and *in vivo*. The dimension of wormlike micelles, tubes, discs and stomatocytes is another concern since many of them are long (from hundreds to thousands of nanometers) or too large. It would be more interesting if there is a robust method to fabricate short wormlike micelles and tubes or small-sized discs and stomatocytes based on well-accepted biodegradable and biocompatible materials such as polylactide and poly(ε-caprolactone). Given the fact that most shaped nanoparticles are only used as a model system, which is not optimal for cancer therapy in terms of materials and/or dimension, so far there is no report on biosafety studies for shaped polymeric nanosystems, which is vital for clinical applications. Moreover, most of the shaped nanoparticles have no active targeting ligands. However, to achieve selective uptake by target tumor cells and precision cancer chemotherapy, active targeting is of critical importance. Last but not least, most shaped nanoparticles reveal low drug loading efficacy and sustained release profile. For clinical translation, drug encapsulation in shaped nanoparticles has to be improved. Furthermore, to potentiate their antitumor efficacy, tumor microenvironment-sensitive nanoparticles that trigger drug release at the target site are desired. In conclusion, there remain many scientific challenges for shaped nanomedicines in cancer therapy ranging from design, fabrication and characterization to *in vitro* and *in vivo* validation.

Acknowledgements

Authors acknowledge support from the National Natural Science Foundation of China (NSFC 51561135010, 51773146, 51633005), the Dutch Ministry of Education, Culture and Science (Gravitation program 024.001.035), NWO-NSFC Advanced Materials (project 792.001.015), the ERC Advanced grant Artisym (694120), and the European Union's Horizon 2020 research and innovation programme Marie Skłodowska-Curie Innovative Training Networks (ITN) Nanomed, under grant No. 676137 for funding. DSW thanks the Ser Cymru II programme for support; this project received funding from the European Union's Horizon 2020 research and innovation under the Marie Skłodowska-Curie grant agreement No. 663830.

References

[1] D.S. Williams, I.A.B. Pijpers, R. Ridolfo, J.C.M. van Hest, *J. Control. Release*. **2017**, *259*, 29–39.

[2] Y. Barenholz, *J. Control. Release*. **2012**, *160*, 117–134.

[3] A. Wicki, D. Witzigmann, V. Balasubramanian, J. Huwyler, *J. Control. Release*. **2015**, *200*, 138–157.

[4] D.E. Owens, N.A. Peppas, *Int. J. Pharm.* **2006**, *307*, 93–102.

[5] S.-D. Li, L. Huang, *Journalf Con*. **2011**, *145*, 178–181.

[6] L. Tang, X. Yang, Q. Yin, K. Cai, H. Wang, I. Chaudhury, C. Yao, Q. Zhou, M. Kwon, J.A. Hartman, I.T. Dobrucki, L.W. Dobrucki, L.B. Borst, S. Lezmi, W.G. Helferich, A.L. Ferguson, T.M. Fan, J. Cheng, *Proc. Natl. Acad. Sci.* **2014**, *111*, 15344–15349.

[7] E. Blanco, H. Shen, M. Ferrari, *Nat. Biotechnol.* **2015**, *33*, 941–951.

[8] N. Doshi, A.S. Zahr, S. Bhaskar, J. Lahann, S. Mitragotri, *Proc. Natl. Acad. Sci. U. S. A.* **2009**, *106*, 21495–21499.

[9] H. Maeda, J. Wu, T. Sawa, Y. Matsumura, K. Hori, *J. Control. Release*. **2000**, *65*, 271–284.

[10] N. Bertrand, J. Wu, X. Xu, N. Kamaly, O.C. Farokhzad, *Adv. Drug Deliv. Rev.* **2014**, *66*, 2–25.

[11] T. Lammers, F. Kiessling, W.E. Hennink, G. Storm, *J. Control. Release*. **2012**, *161*, 175–187.

[12] W. Jiang, B.Y.S. Kim, J.T. Rutka, W.C.W. Chan, *Nat. Nanotechnol.* **2008**, *3*, 145–150.

[13] V.P. Chauhan, Z. Popović, O. Chen, J. Cui, D. Fukumura, M.G. Bawendi, R.K. Jain, *Angew. Chemie - Int. Ed.* **2011**, *50*, 11417–11420.

[14] H.-P.M. de Hoog, M. Nallani, N. Tomczak, *Soft Matter*. **2012**, *8*, 4552–4561.

[15] D.H. Levine, P.P. Ghoroghchian, J. Freudenberg, G. Zhang, M.J. Therien, M.I. Greene, D.A. Hammer, R. Murali, *Methods*. **2008**, *46*, 25–32.

[16] F. Wang, J. Xiao, S. Chen, H. Sun, B. Yang, J. Jiang, X. Zhou, J. Du, *Adv. Mater.* **2018**, *30*, 1–8.

[17] X. Zhang, P. Tanner, A. Graff, C.G. Palivan, W. Meier, *J. Polym. Sci. Part A Polym. Chem.*

2012, *50*, 2293–2318.
[18] D. Discher, A. Eisenberg, *Science*. **2005**, *297*, 967–974.
[19] B.L. Banik, P. Fattahi, J.L. Brown, *Wiley Interdiscip. Rev. Nanomedicine Nanobiotechnology*. **2016**, *8*, 271–299.
[20] R. Salva, J.F. Le Meins, O. Sandre, A. Bruîlet, M. Schmutz, P. Guenoun, S. Lecommandoux, *ACS Nano*. **2013**, *7*, 9298–9311.
[21] X. Sui, P. Kujala, G.-J. Janssen, E. de Jong, I.S. Zuhorn, J.C.M. van Hest, *Polym. Chem.* **2015**, *6*, 691–696.
[22] A. Koide, A. Kishimura, K. Osada, W.D. Jang, Y. Yamasaki, K. Kataoka, *J. Am. Chem. Soc.* **2006**, *128*, 5988–5989.
[23] C.G. Palivan, R. Goers, A. Najer, X. Zhang, A. Car, W. Meier, *Chem. Soc. Rev.* **2016**, *45*, 377–411.
[24] F. Ahmed, D.E. Discher, *J. Control. Release*. **2004**, *96*, 37–53.
[25] J. Gaitzsch, X. Huang, B. Voit, *Chem. Rev.* **2015**, *116*, 1053–1093.
[26] D.E. Discher, F. Ahmed, *Annu. Rev. Biomed. Eng.* **2006**, *8*, 323–341.
[27] X. Hu, Y. Zhang, Z. Xie, X. Jing, A. Bellotti, Z. Gu, *Biomacromolecules*. **2017**, *18*, 649–673.
[28] J.H. Ryu, R. Roy, J. Ventura, S. Thayumanavan, *Langmuir*. **2010**, *26*, 7086–7092.
[29] H.J. Li, J.Z. Du, J. Liu, X.J. Du, S. Shen, Y.H. Zhu, X. Wang, X. Ye, S. Nie, J. Wang, *ACS Nano*. **2016**, *10*, 6753–6761.
[30] C. Wong, T. Stylianopoulos, J. Cui, J. Martin, V.P. Chauhan, W. Jiang, Z. Popovic, R.K. Jain, M.G. Bawendi, D. Fukumura, *Proc. Natl. Acad. Sci.* **2011**, *108*, 2426–2431.
[31] Y. Li, X. Xu, X. Zhang, Y. Li, Z. Zhang, Z. Gu, *ACS Nano*. **2017**, *11*, 416–429.
[32] Q. Lei, S.B. Wang, J.J. Hu, Y.X. Lin, C.H. Zhu, L. Rong, X.Z. Zhang, *ACS Nano*. **2017**, *11*, 7201–7214.
[33] M. Ye, Y. Han, J. Tang, Y. Piao, X. Liu, Z. Zhou, J. Gao, J. Rao, Y. Shen, *Adv. Mater.* **2017**, *29*, 1–10.
[34] J. Li, K. Wei, S. Zuo, Y. Xu, Z. Zha, W. Ke, H. Chen, Z. Ge, *Adv. Funct. Mater.* **2017**, *27*, 1–13.
[35] D. Huo, S. Liu, C. Zhang, J. He, Z. Zhou, H. Zhang, Y. Hu, *ACS Nano*. **2017**, *11*, 10159–10174.
[36] R. Tong, H.D. Hemmati, R. Langer, D.S. Kohane, *J. Am. Chem. Soc.* **2012**, *134*, 8848–8855.
[37] A. Larrañaga, M. Lomora, J.R. Sarasua, C.G. Palivan, A. Pandit, *Prog. Mater. Sci.* **2017**, *90*, 325–357.
[38] K.T. Kim, J.J.L.M. Cornelissen, R.J.M. Nolte, J.C.M. Van Hest, *Adv. Mater.* **2009**, *21*, 2787–2791.
[39] J. Li, Y. Li, Y. Wang, W. Ke, W. Chen, W. Wang, Z. Ge, *Nano Lett.* **2017**, *17*, 6983–6990.
[40] J. a Champion, Y.K. Katare, S. Mitragotri, *Proc. Natl. Acad. Sci. U. S. A.* **2007**, *104*, 11901–4.

[41] J.A. Champion, Y.K. Katare, S. Mitragotri, *J. Control. Release*. **2007**, *121*, 3–9.
[42] J. a Champion, S. Mitragotri, *Proc. Natl. Acad. Sci. U. S. A.* **2006**, *103*, 4930–4934.
[43] J.L. Perry, K.P. Herlihy, M.E. Napier, J.M. Desimone, *Acc. Chem. Res.* **2011**, *44*, 990–998.
[44] S.E. a Gratton, P. a Ropp, P.D. Pohlhaus, J.C. Luft, V.J. Madden, M.E. Napier, J.M. DeSimone, *Proc. Natl. Acad. Sci. U. S. A.* **2008**, *105*, 11613–11618.
[45] J.D. Robertson, G. Yealland, M. Avila-Olias, L. Chierico, O. Bandmann, S.A. Renshaw, G. Battaglia, *ACS Nano*. **2014**, *8*, 4650–4661.
[46] L.K.E.A. Abdelmohsen, D.S. Williams, J. Pille, S.G. Ozel, R.S.M. Rikken, D.A. Wilson, J.C.M. Van Hest, *J. Am. Chem. Soc.* **2016**, *138*, 9353–9356.
[47] I.A.B. Pijpers, L.K.E.A. Abdelmohsen, D.S. Williams, J.C.M. Van Hest, *ACS Macro Lett.* **2017**, *6*, 1217–1222.
[48] K.T. Kim, S. a Meeuwissen, R.J.M. Nolte, J.C.M. van Hest, *Nanoscale*. **2010**, *2*, 844–858.
[49] S.A. Meeuwissen, K.T. Kim, Y. Chen, D.J. Pochan, J.C.M. Van Hest, *Angew. Chemie - Int. Ed.* **2011**, *50*, 7070–7073.
[50] D.A. Wilson, R.J.M. Nolte, J.C.M. van Hest, *Nat. Chem.* **2012**, *4*, 268–274.
[51] L.K.E.A. Abdelmohsen, M. Nijemeisland, G.M. Pawar, G.J.A. Janssen, R.J.M. Nolte, J.C.M. Van Hest, D.A. Wilson, *ACS Nano*. **2016**, *10*, 2652–2660.
[52] B.C. Buddingh', J.C.M. van Hest, *Acc. Chem. Res.* **2017**, *50*, 769–777.
[53] R. Deng, M.J. Derry, C.J. Mable, Y. Ning, S.P. Armes, *J. Am. Chem. Soc.* **2017**, *139*, 7616–7623.
[54] Y. Guo, S. Zhao, H. Qiu, T. Wang, Y. Zhao, M. Han, Z. Dong, X. Wang, *Bioconjug. Chem.* **2018**, *29*, 1302–1311.
[55] B. Godin, C. Chiappini, S. Srinivasan, J.F. Alexander, K. Yokoi, M. Ferrari, P. Decuzzi, X. Liu, *Adv. Funct. Mater.* **2012**, *22*, 4225–4235.
[56] Z. Zhang, X. Wang, B. Li, Y. Hou, Z. Cai, J. Yang, Y. Li, *RSC Adv.* **2018**, *8*, 3274–3285.
[57] T. Hyeon, V. Rotello, *Chem. Soc. Rev.* **2012**, *41*, 2545–2561.
[58] S. Venkataraman, J.L. Hedrick, Z.Y. Ong, C. Yang, P.L.R. Ee, P.T. Hammond, Y.Y. Yang, *Adv. Drug Deliv. Rev.* **2011**, *63*, 1228–1246.
[59] M.J. Ernsting, M. Murakami, A. Roy, S.D. Li, *J. Control. Release*. **2013**, *172*, 782–794.
[60] B. Yameen, W. Il Choi, C. Vilos, A. Swami, J. Shi, O.C. Farokhzad, *J. Control. Release*. **2014**, *190*, 485–499.
[61] S.Y. Lin, W.H. Hsu, J.M. Lo, H.C. Tsai, G.H. Hsiue, *J. Control. Release*. **2011**, *154*, 84–92.
[62] S. Dasgupta, T. Auth, G. Gompper, *Nano Lett.* **2014**, *14*, 687–693.
[63] R. Vácha, F.J. Martinez-Veracoechea, D. Frenkel, *Nano Lett.* **2011**, *11*, 5391–5395.
[64] Y. He, K. Park, *Mol. Pharm.* **2016**, *13*, 2164–2171.
[65] N. Luo, J.K. Weber, S. Wang, B. Luan, H. Yue, X. Xi, J. Du, Z. Yang, W. Wei, R. Zhou, G. Ma, *Nat. Commun.* **2017**, *8*, 1–10.

[66] P. Kolhar, A.C. Anselmo, V. Gupta, K. Pant, B. Prabhakarpandian, E. Ruoslahti, S. Mitragotri, *Proc. Natl. Acad. Sci.* **2013**, *110*, 10753–10758.
[67] Y. Geng, P. Dalhaimer, S. Cai, R. Tsai, M. Tewari, T. Minko, D.E. Discher, *Nat. Nanotechnol.* **2007**, *2*, 249–55.
[68] J. Zhao, H. Lu, P. Xiao, M.H. Stenzel, *ACS Appl. Mater. Interfaces*. **2016**, *8*, 16622–16630.
[69] T. Yue, X. Zhang, *ACS Nano*. **2012**, *6*, 3196–3205.
[70] S.C. Lee, C. Kim, I.C. Kwon, H. Chung, S.Y. Jeong, *J. Control. Release*. **2003**, *89*, 437–446.
[71] V. V. Shuvaev, M.A. Ilies, E. Simone, S. Zaitsev, Y. Kim, S. Cai, A. Mahmud, T. Dziubla, S. Muro, D.E. Discher, V.R. Muzykantov, *ACS Nano*. **2011**, *5*, 6991–6999.
[72] P. Dalhaimer, A.J. Engler, R. Parthasarathy, D.E. Discher, *Biomacromolecules*. **2004**, *5*, 1714–1719.
[73] P.R. Nair, S.A. Karthick, K.R. Spinler, M.R. Vakili, A. Lavasanifar, D.E. Discher, *Nanomedicine (Lond).* **2016**, *11*, 1551–1569.
[74] X. Yi, X. Shi, H. Gao, *Phys. Rev. Lett.* **2011**, *107*, 1–5.
[75] M. Raatz, R. Lipowsky, T.R. Weikl, *Soft Matter*. **2014**, *10*, 3570–3577.
[76] H. Cabral, Y. Matsumoto, K. Mizuno, Q. Chen, M. Murakami, M. Kimura, Y. Terada, M.R. Kano, K. Miyazono, M. Uesaka, N. Nishiyama, K. Kataoka, *Nat. Nanotechnol.* **2011**, *6*, 815–823.
[77] J. Sun, L. Zhang, J. Wang, Q. Feng, D. Liu, Q. Yin, D. Xu, Y. Wei, B. Ding, X. Shi, X. Jiang, *Adv. Mater.* **2015**, *27*, 1402–1407.
[78] F. Meng, Z. Zhong, J. Feijen, *Biomacromolecules*. **2009**, *10*, 197–209.
[79] K. Kostarelos, L. Lacerda, G. Pastorin, W. Wu, S. Wieckowski, J. Luangsivilay, S. Godefroy, D. Pantarotto, J.P. Briand, S. Muller, M. Prato, A. Bianco, *Nat. Nanotechnol.* **2007**, *2*, 108–113.
[80] A.E. Porter, M. Gass, K. Muller, J.N. Skepper, P.A. Midgley, M. Welland, *Nat. Nanotechnol.* **2007**, *2*, 713–717.
[81] R. Singh, D. Pantarotto, L. Lacerda, G. Pastorin, C. Klumpp, M. Prato, A. Bianco, K. Kostarelos, *Proc. Natl. Acad. Sci.* **2006**, *103*, 3357–3362.
[82] J.D. Robertson, G. Yealland, M. Avila-Olias, L. Chierico, O. Bandmann, S.A. Renshaw, G. Battaglia, *ACS Nano*. **2014**, *8*, 4650–4661.
[83] C. Pegoraro, D. Cecchin, L.S. Gracia, N. Warren, J. Madsen, S.P. Armes, A. Lewis, S. MacNeil, G. Battaglia, *Cancer Lett.* **2013**, *334*, 328–337.
[84] H. Lomas, I. Canton, S. MacNeil, J. Du, S.P. Armes, A.J. Ryan, A.L. Lewis, G. Battaglia, *Adv. Mater.* **2007**, *19*, 4238–4243.
[85] G. Yealland, G. Battaglia, O. Bandmann, H. Mortiboysb, *Neurosci. Lett.* **2016**, 23–29.
[86] T. Yue, Y. Xu, M. Sun, X. Zhang, F. Huang, *Phys. Chem. Chem. Phys.* **2016**, *18*, 1082–1091.
[87] J. Varshosaz, F. Hassanzadeh, H.S. Aliabadi, M. Banitalebi, M. Rostami, M. Nayebsadrian,

Colloid Polym. Sci. **2014**, *292*, 2647–2662.
[88] Y.C. Wang, F. Wang, T.M. Sun, J. Wang, *Bioconjug. Chem.* **2011**, *22*, 1939–1945.
[89] N.S. Lee, L.Y. Lin, W.L. Neumann, J.N. Freskos, A. Karwa, J.J. Shieh, R.B. Dorshow, K.L. Wooley, *Small*. **2011**, *7*, 1998–2003.
[90] S. Cai, K. Vijayan, D. Cheng, E.M. Lima, D.E. Discher, *Pharm. Res.* **2007**, *24*, 2099–2109.
[91] J. Eliezar, W. Scarano, N.R.B. Boase, K.J. Thurecht, M.H. Stenzel, *Biomacromolecules*. **2015**, *16*, 515–523.
[92] S.C. Owen, D.P.Y. Chan, M.S. Shoichet, *Nano Today*. **2012**, *7*, 53–65.
[93] C. Deng, Y. Jiang, R. Cheng, F. Meng, Z. Zhong, *Nano Today*. **2012**, *7*, 467–480.
[94] J.O. Lee, K.T. Oh, D. Kim, E.S. Lee, *J. Mater. Chem. B*. **2014**, *2*, 6363–6370.
[95] D. Li, Z. Tang, Y. Gao, H. Sun, S. Zhou, *Adv. Funct. Mater*. **2016**, *26*, 66–79.
[96] A. Gabizon, H. Shmeeda, Y. Barenholz, *Clin.Pharmacokinet.* **2003**, *42*, 419–436.
[97] A.K. Iyer, G. Khaled, J. Fang, H. Maeda, *Drug Discov. Today*. **2006**, *11*, 812–818.
[98] H.F. Dvorak, *Prog. Clin. Biol. Res.* **1990**, *354A*, 317—330.
[99] C. Link, F. Alexis, E. Pridgen, L.K. Molnar, *Mol. Pharm.* **2008**, *5*, 505–515.
[100] B.R. Smith, P. Kempen, D. Bouley, A. Xu, Z. Liu, N. Melosh, H. Dai, R. Sinclair, S.S. Gambhir, *Nano Lett.* **2012**, *12*, 3369–3377.
[101] K.K. Ng, J.F. Lovell, A. Vedadi, T. Hajian, G. Zheng, *ACS Nano*. **2013**, *7*, 3484–3490.